

Inter-comparison of OC-CCI chlorophyll-a estimates with precursor data sets

André Belo Couto, Vanda Brotas, Frédéric Mélin, Steve Groom & Shubha Sathyendranath

To cite this article: André Belo Couto, Vanda Brotas, Frédéric Mélin, Steve Groom & Shubha Sathyendranath (2016) Inter-comparison of OC-CCI chlorophyll-a estimates with precursor data sets, International Journal of Remote Sensing, 37:18, 4337-4355, DOI: 10.1080/01431161.2016.1209313

To link to this article: <http://dx.doi.org/10.1080/01431161.2016.1209313>



Published online: 25 Jul 2016.



Submit your article to this journal [↗](#)



View related articles [↗](#)



View Crossmark data [↗](#)



Inter-comparison of OC-CCI chlorophyll-*a* estimates with precursor data sets

André Belo Couto ^a, Vanda Brotas^a, Frédéric Mélin^b, Steve Groom^c
and Shubha Sathyendranath^c

^aMARE – Marine and Environmental Sciences Centre, Faculdade de Ciências, Universidade de Lisboa, Lisboa, Portugal; ^bEuropean Commission, Joint Research Centre (JRC), Institute for Environment and Sustainability (IES), Ispra, Italy; ^cPlymouth Marine Laboratory, Prospect Place, The Hoe, Plymouth, UK

ABSTRACT

Ocean colour is the only essential climate variable that targets a biological variable (chlorophyll-*a* concentration (chl-*a*)) and is also amenable to remote sensing at the global scale. However, the finite lifetime of individual ocean-colour sensors, and the differences in their characteristics increase the difficulty of creating a long-term, consistent, ocean-colour time series that meets the requirements of climate studies. The Ocean Colour Climate Change Initiative (OC-CCI), a European Space Agency programme, has recently produced a time series of satellite-based ocean-colour products at the global scale, merging data from three sensors: Sea-viewing Wide Field-of-view Sensor (SeaWiFS), Moderate Resolution Imaging Spectroradiometer on the Aqua Earth Observing System (MODIS-Aqua), and Medium Resolution Imaging Spectrometer (MERIS), while attempting to reduce inter-sensor biases. In this work we present a comparison between the OC-CCI chlorophyll-*a* product and precursor satellite-derived data sets, from both single missions (SeaWiFS, MODIS-Aqua, and MERIS) and multi-mission products (global ocean colour (GlobColour) and Making Earth Science Data Records for Use in Research Environments (MEaSUREs)). To this end, OC-CCI global monthly composites are compared to the similar products offered by single-mission and multi-mission records. Our results indicate that the OC-CCI product provides a higher number of observations. Comparing the observations that match with precursors, the OC-CCI product was generally most similar to the single-mission products. Relationships between OC-CCI and other precursors did not change significantly during a common and continuous period, and, on average the root-mean-square differences between log-transformed chlorophyll-*a* concentration are below or equal to 0.11. Further, when considering variability that could arise when merging data from different sources, it is shown that the OC-CCI product is a longer term constant than those from other multi-mission initiatives studied here.

ARTICLE HISTORY

Received 20 July 2015
Accepted 17 June 2016

1. Introduction

Climate change is arguably the greatest environmental challenge for the twenty-first century, and evidence that anthropogenic activity is forcing a shift in natural climate variability is more robust than ever (IPCC 2013). To provide information on the state of the global climate system and its variability, the Global Climate Observing System (GCOS) has listed (GCOS 2011), amongst other variables, the oceanic near-surface chlorophyll-*a* concentration (chl-*a*) derived from ocean colour (OC) radiometry (Figure 1) as an essential climate variable (ECV). Chlorophyll plays a crucial role in photosynthesis within phytoplankton cells; furthermore, the benefits of recording global oceanic chl-*a* are extended to climate monitoring, knowledge of the carbon cycle, including exchanges between ocean and atmosphere, as well as providing an ecological indicator of the marine environment and mapping of marine ecological provinces (GCOS 2011). Several publications have discussed the dynamics of chlorophyll due to climate variability. For instance, Yoder and Kennelly (2003) demonstrated that the seasonal cycle was responsible for most of the variability in a 4-year near-global data set, whilst Behrenfeld et al. (2006) demonstrated that inter-annual variability in global chlorophyll-*a* patterns is linked to El Niño Southern Oscillation (ENSO) variability. Couto, Holbrook, and Maharaj (2013) further suggested that multi-annual to decadal chl-*a* variability depends on the dominant flavour of ENSO, and Brewin et al. (2012) highlighted the impact of Indian Ocean Dipole on phytoplankton size structure inferred from chlorophyll-*a*. However, available chlorophyll records are restricted in their capacity to assess response to climate changes (Henson et al. 2010), either due to a limited spatial coverage (when based on *in situ* data), or short temporal span (for remote-sensing data).

In this article we focus on the remote-sensing approach to study chlorophyll variability in the global ocean. Since the launch of the Coastal Zone Color Scanner (CZCS) in the late 1970s, the first ocean colour sensor on an Earth orbiting satellite platform, several other ocean-colour sensors have been launched that have provided observations of regional-to-global chl-*a* data. However, longevity of such sensors is about a decade at best, making each mission by itself unsuitable to assess impact of climate shift on chlorophyll-*a*. To extend the time series beyond that provided by single satellite sensors,

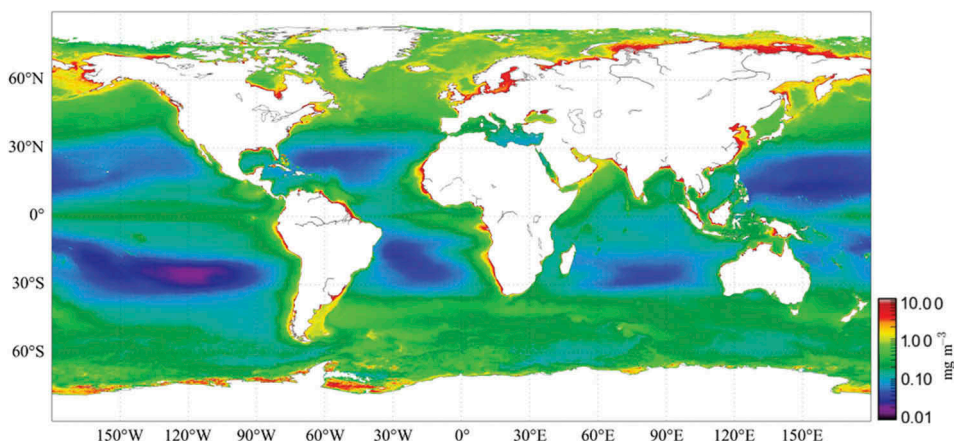


Figure 1. Multiannual average of chlorophyll-*a* global distribution (OC-CCI V1.0).

Ocean Colour – Climate Change Initiative (OC-CCI) of the European Space Agency (ESA) has generated multi-sensor, global, ocean-colour products for climate research by merging observations from three different sensors, the Sea-viewing Wide Field-of-view Sensor (SeaWiFS), the Moderate Resolution Imaging Spectroradiometer on board the Aqua Earth Observing System (MODIS-Aqua), and, the Medium Resolution Imaging Spectrometer (MERIS) (Storm et al. 2013). The merging process consisted in correcting the differences between the band wavelengths observed from the different sensors to a common set of bands (the ones from SeaWiFS), before merging observations and computing the final products (further details are provided in Section 2 of this article, and by Mélin and Sclep 2015). The processing adopted strove for completeness in coverage and consistency across sensors.

Comparing any new ocean-colour data set to single mission data and other precursor data sets is an integral part of quality control. Such exercise provides information needed for the user community to relate the new product with other products available. Additionally, it contributes to gain some insight on the uncertainties affecting these products, to the extent they are revealed by inter-comparison. The main goal of this article is to assess the similarity of OC-CCI chl-*a* product with other existing satellite-derived data sets, and any instabilities in the OC-CCI products that can arise from merging multi-mission observations.

2. Data

The data sets used in this study comprise chl-*a* estimates derived from individual satellite missions and multi-mission merged data sets as well as a sea surface temperature (SST) record. There are only a few satellite sensors that provide the scientific community with a multi-year series of ocean colour (OC) global observations (www.ioccg.org/sensors/current.html). Further, there are a few data sets where the available OC observations were merged to create a more complete record. Properties of the different remotely sensed data sets are summarized in Table 1. All data sets were global gridded monthly composites at 4.6 km resolution, with the exception of the SeaWiFS and MEaSUREs products, which are delivered with 9.2 km grid resolution. The monthly composites provide fairly complete global coverage while retaining a good description of the annual cycle.

The single mission data sets used in this study were SeaWiFS, MODIS-Aqua, and MERIS, widely used in peer-reviewed literature (e.g. Behrenfeld et al. 2006; Djavidnia, Mélin, and Hoepffner 2010; Couto, Holbrook, and Maharaj 2013; Sá et al. 2015) and are

Table 1. Properties of the data sets used.

Data sets	Individual missions			Merged products				
	SeaWiFS*	MERIS	MODIS-Aqua	GC-GSM	GC-AVW	MEaSUREs	OC-CCI	SST
Temporal coverage	Start	Sep-97	Apr-02	Jul-02	Sep-97	Sep-97	Sep-97	Sep-97
	End	Dec-10	Apr-12	Jul-12	Jul-12	Jul-12	Jul-12	Jul-12
Data set version	R2010.0	R2012.1	R2013.0	-	-	V6 and V7	V1.0	V5.2
Chl- <i>a</i> algorithm	OC4v6	OC4Ev6	OC3Mv6	GSM	Average	GSM	OC4v6	N/A
Spatial resolution (km ²)	9.0	4.6	4.6	4.6	4.6	9.2	4.6	4.6
Temporal resolution	Monthly	Monthly	Monthly	Monthly	Monthly	Monthly	Monthly	Monthly

* SeaWiFS record has a gap of data from 01.2008 to 03.2008, for 07.2008, 05.2009, 09.2009, and 10.2009.

easily accessed. The characteristics of these data sets are described in Table 1, and were retrieved from the National Aeronautics and Space Administration (NASA) Ocean Colour website (<http://oceandata.sci.gsfc.nasa.gov/>). In the NASA processing chain, remote-sensing reflectance is first obtained following a common atmospheric correction procedure (Franz et al. 2007), to which various versions of the ocean colour algorithm proposed by O'Reilly et al. (2000) were applied. Data were retrieved from the source in a global cylindrical projection.

Merged data sets combine data from different individual missions to create time series with increased temporal and spatial coverage. When combining information derived from three ocean-colour missions, processed with different algorithms, differences arise from the merging techniques and versions of algorithms used. Only a few data sets that merge global OC observations from different sensors are available, and, to our knowledge, all are included herein: the Global ocean Colour (GlobColour) project products funded (2005–2008) by the European Space Agency (www.globcolour.info); the Making Earth Science Data Records for Use in Research Environments (MEaSUREs) initiative supported by NASA (2006, 2012) and available from the University of California in Santa Barbara (wiki.icess.ucsb.edu/measures/); and, version 1 of the OC-CCI project funded (2010–2017) by ESA (www.esa-oceancolour-cci.org/).

GlobColour (GC) provided two data sets: the weighted average (GC-AVW) and the Garver–Siegel–Maritorena (GC-GSM) data sets. The two GC data sets differ in the merging techniques used, and the algorithms used for chl-*a* concentrations retrieval. For the GC-AVW data set, daily chl-*a* products were computed using the level-2 data from each source, and then the chl-*a* values derived from SeaWiFS and MODIS were adjusted as in Morel et al. (2007) to get values compatible with MERIS data (GlobColour 2010). The merged product was then generated by averaging level-3 products using the number of observations from each sensor as the weights. For the GC-GSM data set, the daily level-3 fully normalized water-leaving radiances from SeaWiFS, MODIS-Aqua, and MERIS are used simultaneously in GSM, a semi-analytical ocean colour inversion algorithm (Maritorena, Siegel, and Peterson 2002; Maritorena and Siegel 2005; Maritorena et al. 2010) that produces chlorophyll concentrations. For both GC data sets, reprocessing NASA R2005.1 was used for SeaWiFS and MODIS-Aqua (GlobColour 2010). For MERIS, data are based on the second reprocessing (that relies on the MEGS-7 atmospheric correction) between April 2002 and July 2011, and on the third reprocessing (that relies on the MERIS Ground Segment data processing prototype 8 (MEGS-8) atmospheric correction) between August 2011 and July 2012 (MERIS Quality Working Group 2011). Both GC data sets were obtained in a global binned sinusoidal grid format, with average width of 4.6 km, an area equivalent to 21.44 km²; the poles are represented by three bins, in a mesh with 8640 columns and 4320 rows (GlobColour 2010). GC data were obtained in May 2014.

The MEaSUREs chl-*a* is also derived using the GSM model, similar to the previously described GC-GSM product. However, unlike the latter, for MEaSUREs MODIS-Aqua and MERIS level 3 binned, normalized, water-leaving radiances were first mapped on a 9.2 km grid to match the resolution of SeaWiFS. Further, MEaSUREs used a more limited number of wavebands than GC-GSM (see Maritorena et al. 2010 for more details), more recent reprocessing versions of satellite data (SeaWiFS R.2010.0, MODIS-Aqua R2012.0

and MERIS V3.1) and all MERIS data were processed using the ESA MEGS-8 processor. MEaSUREs data were obtained in July 2014.

The ESA OC-CCI version 1.0 data set differed from the other merged products in the versions of satellite data and algorithms used and in the merging process. SeaWiFS and MODIS processing versions were NASA versions R2010.0 and R2013.0, respectively, the same as the corresponding single-mission data sets described above. For MERIS atmospheric correction, the POLYnomial-based algorithm applied to MERIS (POLYMER) was used (Steinmetz, Deschamps, and Ramon 2011).

OC-CCI is a product (Figure 1) constructed using SeaWiFS as a reference in many of its aspects. The reasons for this choice are that SeaWiFS is widely considered to be the highest quality sensor with the best match to *in situ* observations, besides being commonly used in peer literature. The band-shifting and bias-correction processes are crucial steps within the OC-CCI production chain. The spectral values of remote-sensing reflectance (R_{rs}) obtained after atmospheric correction of MODIS and MERIS data were shifted to the nearest SeaWiFS bands (412, 443, 490, 510, 555, and 670 nm) using a band-shifting approach that is based on an ocean-colour bio-optical model (Mélin and Sclep 2015). Sensor-specific bias-correction is a crucial step in the OC-CCI process, since it guarantees the inter-sensor consistency by correcting deviations of the quality of the observations during the period of activity. These deviations may unfold as temporal and spatial artefacts in the final product (e.g. Djavidnia, Mélin, and Hoepffner 2010). In the context of the OC-CCI, a bias-correction method is applied to reduce inter-sensor-bias. This is done by applying a multi-annual bias-correcting ratio to each pixel of the band-shifted MODIS-Aqua and MERIS R_{rs} (while SeaWiFS data are used as a reference), where this ratio is calculated with multi-annual averages obtained from the period 2003–2007 common to all three records (Mélin 2014; Mélin and Sclep 2015). Hence, this process brings MODIS-Aqua and MERIS data closer to the SeaWiFS observations. Band-shifting, bias-correction, and merging processes are done with level-3 binned data. This merging approach generated a set of R_{rs} values at (SeaWiFS) wavebands, which allowed a common chlorophyll algorithm to be applied to the merged data (Mélin 2014). OC-CCI uses the OC4V6 (NASA 2010; O'Reilly et al. 2000) algorithm to retrieve chl-*a* concentrations, which is the same algorithm as the SeaWiFS data set. The OC-CCI data set includes a higher number of observations from MERIS than in other merged products, because the POLYMER atmospheric correction retrieves more R_{rs} values in challenging conditions (sun glint, thin clouds, or aerosols) than the SeaWiFS Data Analysis System (SeaDAS) or the MEGS processors (Steinmetz, Deschamps, and Ramon 2011), hence OC-CCI presents a better spatial coverage than other merged products. The OC-CCI product was retrieved on an equidistant cylindrical geographic grid from the project website (<http://www.esa-oceancolour-cci.org/>), where latitude and longitude are converted directly to a rectangular grid with 8640 columns and 4320 rows. OC-CCI data were obtained in July 2013.

The Pathfinder program has been compiling global satellite-derived Sea Surface Temperature (SST) data for more than 30 years (Casey et al. 2010), gathering observations from several generations of the Advanced Very High Resolution Radiometers (AVHRR) on board satellites operated by the National Oceanic and Atmospheric Administration (NOAA). The current version of the Pathfinder SST data (V5.2) was obtained from the National Oceanographic Data Center (www.nodc.noaa.gov/SatelliteData/pathfinder4km/) at 4.6 km spatial resolution and a temporal resolution

of 1 day for the same period as the OC-CCI product (September 1997 to July 2012). These global SST maps were averaged to monthly composites, matching the spatial and temporal resolution of the ocean-colour-derived chl-*a* data sets used in this study.

3. Methods

In this work, OC-CCI global chlorophyll-*a* monthly composites are compared, grid point by grid point, with the similar record of the precursor data sets. As explained above, not all data sets have the same spatial resolution. Actually, only two data sets (SeaWiFS and MEaSUREs) have a grid twice coarser than the other sets, which are in turn all on the same grid. To be able to compare all records against the OC-CCI product, prior to the analysis, SeaWiFS and MEaSUREs records were mapped onto the same grid as that of the OC-CCI, using a linear interpolation approach. This might introduce additional differences between compared records with respect to a hypothetical comparison with a SeaWiFS /MEaSUREs 4.6-km data set. Nevertheless, we do not expect a major factor, since the results obtained in the comparison between OC-CCI and SeaWiFS /MEaSUREs are well in line with the other comparisons (actually statistics for SeaWiFS are of a closer agreement). Pairs of all matched observations were selected for each of the data sets compared. Statistical metrics were calculated to evaluate the differences between data sets including: the bias (δ), unbiased root mean square (RMS) difference ($\Delta_{u,RMS}$), mean ratio (ϕ) and correlation coefficient (r), which are metrics commonly used for comparison and evaluation of products in this field (e.g. IOCCG 2006). Here, rather than calculate the RMS difference (Δ_{RMS}), we calculated the unbiased RMS difference ($\Delta_{u,RMS}$) instead, as it provides the unbiased component of the total RMS difference. The analyses were carried out for two periods: first, for a period common to all data sets with continuous observations, that is, no gaps in the monthly composite record (2003–2007, inclusive), that aimed to assess the similarity between each record; and second for periods common to any pair of data sets. chl-*a* values of all data sets were \log_{10} -transformed before the analysis, because of the log-normal distribution of satellite-derived chlorophyll data at the global scale. The quantities δ and $\Delta_{u,RMS}$ are, therefore, relative values of the untransformed data (Gregg and Casey 2004):

$$\delta = \frac{1}{N} \sum_{i=1}^N [\log_{10}(C_{2,i}) - \log_{10}(C_{1,i})], \quad (1)$$

where N represents the total number of matched observations (i) in a monthly global map, between C_1 and C_2 (in this study C_1 represents the OC-CCI product, and C_2 any other data set). The $\Delta_{u,RMS}$ (unbiased RMS difference) with the same units as chl-*a*, is defined as (Jolliff et al. 2009):

$$\Delta_{u,RMS} = \left(\frac{1}{N} \sum_{i=1}^N \left\{ \left[\log_{10}(C_{2,i}) - \overline{\log_{10}(C_{2,i})} \right] - \left[\log_{10}(C_{1,i}) - \overline{\log_{10}(C_{1,i})} \right] \right\}^2 \right)^{1/2}, \quad (2)$$

where the overbar represents the average. The mean ratio (ϕ) is defined as:

$$\phi = \frac{1}{N} \sum_{i=1}^N \frac{C_{2,i}}{C_{1,i}}, \quad (3)$$

and the correlation coefficient (r) as:

$$r = \frac{\sum_{i=1}^N \left(\log_{10}(C_{1,i}) - \overline{\log_{10}(C_1)} \right) \left(\log_{10}(C_{2,i}) - \overline{\log_{10}(C_2)} \right)}{\left[\sum_{i=1}^N \left(\log_{10}(C_{1,i}) - \overline{\log_{10}(C_1)} \right)^2 \right]^{\frac{1}{2}} \left[\sum_{i=1}^N \left(\log_{10}(C_{2,i}) - \overline{\log_{10}(C_2)} \right)^2 \right]^{\frac{1}{2}}}. \quad (4)$$

3.1. Target, Taylor, and mutual information diagrams

The statistics described above assess the relationships between pairs of data; however, the use of multiple metrics could make interpretation difficult. Target, Taylor, and mutual information diagrams become useful as these combine statistics to summarize results (Jolliff et al. 2009). These have been widely used in recent years in remote sensing and climate research, and their applicability is quite vast (e.g. Djavidnia, Mélin, and Hoepffner 2010).

3.1.1. Target diagram

Target diagram (Jolliff et al. 2009) displays simultaneously, the bias δ and the unbiased RMS difference $\Delta_{u,RMS}$, which is that part of the total RMS difference due to the scatter between points (the total RMS difference being equal to $[\Delta_{u,RMS}^2 + \delta^2]^{1/2}$).

3.1.2. Taylor diagram

The Taylor diagram illustrates four metrics in a single polar plot, exploiting the cosine law that links them (Taylor 2001). These are: the standard deviations of each monthly composite from the pair of data sets compared (σ_{C_1} and σ_{C_2}), which are plotted as the length of the sides of a triangle; the coefficient of correlation r between the pair of monthly composites compared (Equation (4)), which is represented by the cosine of the angle between the two sides in the diagram; and $\Delta_{u,RMS}$, which is given by the length of the opposite side. The Taylor plot (Taylor 2001) is based on the following relationship between each monthly composite from the pair of records compared:

$$\Delta_{u,RMS}^2 = \sigma_{\log_{10}(C_1)}^2 + \sigma_{\log_{10}(C_2)}^2 - 2\sigma_{\log_{10}(C_1)}\sigma_{\log_{10}(C_2)}r, \quad (5)$$

which is identical to Equation (2).

3.1.3. Mutual information diagram

The mutual information diagram (MID) is similar to the Taylor diagram in that it illustrates multiple statistics that share a similar relationship onto a single polar plot. However, MID does so by using a non-linear set of statistics (based on probability) to assess similarity between records, whereas Taylor diagram is based on the assumption of linearity. In MID (Correa and Lindstrom 2013), the properties used are entropy (H), mutual information (I), and the root variation of information (RVI). Entropy was

calculated for each monthly composite as a function of: the probability of each matched observation $p(C_i)$ to have an outcome C_i . Monthly entropy is defined as:

$$H(C) = - \sum_{i=1}^N p(C_i) \log_2(p(C_i)). \quad (6)$$

To calculate probability (p) the histogram of distribution for the chl- a is produced in \log_{10} scale by dividing the data into 50 bins within the interval -2 to 2 (that is chlorophyll range between 0.01 and 100 mg m^{-3}). Mutual information (I), here, is a measure of the information shared between the monthly composites from two different data sets, and is defined as:

$$I(C_1; C_2) = H(C_1) + H(C_2) - H(C_1, C_2), \quad (7)$$

where $H(x, y)$ represents the joint entropy of the monthly composites of C_1 and C_2 data sets:

$$H(C_1, C_2) = \sum_{C_1} \sum_{C_2} P(C_1, C_2) \log_2[P(C_1, C_2)]. \quad (8)$$

$P(C_1, C_2)$ represents the joint probability of values between two data sets (C_1 and C_2) occurring together. Calculating P the histogram of distribution for the chl- a follows the same methodology as p in Equation (6). Normalized mutual information (NI) is then computed from entropy H and mutual information I , as follows:

$$NI = \frac{I}{\sqrt{H(C_1)H(C_2)}}. \quad (9)$$

Correa and Lindstrom (2013) point out further that these properties are related to the root of variation information (RVI) according to the following relationship:

$$RVI(C_1, C_2) = [H(C_1) + H(C_2) - 2(NI)]^{1/2}, \quad (10)$$

which is a metric of similarity between the two variables. Similarly to the Taylor diagram, the MID diagram displays on a single polar plot four statistical metrics, which hold similar relationship to each other as in the Taylor diagram. Correa and Lindstrom (2013) point out some differences and advantages of MID with respect to the Taylor diagram. For example, the quantities represented in the MID are able to capture both linear and non-linear relationships, and are less sensitive to outliers. When the two records compared (x and y) are identical, then the NI would take a maximum score of one, and the RVI would be zero.

For the final diagrams displayed, the described metrics were averaged in time.

The tendency of OC-CCI relationship with precursor records was tested by calculating the trend of each metric temporal-series, after the removal of the mean seasonal cycle, within a common time frame for all records (2003–2007).

3.2. Testing OC-CCI long-term consistency

One of the main objectives of this study was to assess the long-term consistency of the OC-CCI product over time. To assess OC-CCI long-term consistency, ideally OC-CCI would

have to be compared against another chl-*a* record that covers the same period, but does not include the same data. In the absence of such a chl-*a* record, we have used an SST data set for the following reasons:

- SST is a measure of the state of the ocean independent of the OC-CCI chl-*a* product, or any of its sources;
- SST shares a significant and robust relationship with the abundance of chlorophyll in the ocean, since large-scale processes that drive SST variability are also responsible for phytoplankton variability. The relationship that is often observed between SST and chl-*a* is negative, as it illustrates the process of growing phytoplankton (increase of chl-*a* concentration) when deep nutrient-rich waters surface (colder SST);
- The SST data set used here, the Pathfinder, has similar characteristics to those offered by the OC-CCI record. For example, both records provide global measurements of the ocean state during a common time frame that allows inter-comparison. And, to further simplify this comparison, both records share similar temporal and spatial resolutions;
- The Pathfinder data set is a very well known record in ocean and climate science, as it is widely used in peer-reviewed literature for decades.
- Since SST and log-transformed chl-*a* represent two fields with different ranges, each data set was standardized by subtracting the average and dividing by the standard deviation, to allow a dimensionless (i.e. without units) comparison. Note that the standardization removes the bias between data sets.

The variability through time of the unbiased difference between measurements of two different data sets (e.g. $\Delta_{u,RMS}$, Equation (2)) is a measurement indicative of the consistency of both data sets relative to each other. Comparing the standard deviation σ (a measure of variability) of each $\Delta_{u,RMS}$ ($s\Delta_{u,RMS}$) between OC-CCI and the other records, consistency of OC-CCI can be inferred (a smaller $s\Delta_{u,RMS}$ is representative of a more stable relationship).

4. Results

The average number of observations matched between OC-CCI and precursors in a monthly composite (N) was less than 15 million for SeaWiFS and MODIS-Aqua records, above 16 million for MERIS, and above 17 million for all merged products used (Table 2). During the period covered by OC-CCI, that is, September 1997 to July 2012, the number of matched observations increased greatly from the mid-2002 onwards, during the period common to all three single sensors. Before mid-2002, N varies below or just above the 15 million observations per composite when comparing OC-CCI to all single and merged products. After mid-2002, most notably when comparing OC-CCI against the other merged products and the MERIS record, N increased almost reaching the 20 million observations matched between records.

4.1. Similarity of OC-CCI with precursor data sets in a common period

The OC-CCI data set showed little differences with the precursor chl-*a* data within the common time frame (January 2003 to December 2007), when considering only the

Table 2. Statistical results of the comparisons (temporal averaged) between OC-CCI and precursor data sets between a common time frame for all, from January 2003 to December 2007 (for all correlations $p > 0.01$; \bar{N} represents the monthly averaged number of matched observations when comparing against the OC-CCI).

	SeaWiFS	MERIS	MODIS-Aqua	GC-AVW	GC-GSM	MEaSUREs	OC-CCI
ϕ	1.003	0.955	0.972	1.076	1.034	0.954	-
r	0.978	0.972	0.978	0.974	0.958	0.957	-
$\Delta_{u,RMS}$	0.093	0.105	0.096	0.099	0.130	0.130	-
δ	-0.009	-0.033	-0.024	0.019	-0.004	-0.040	-
NI	0.963	0.928	0.941	0.921	0.861	0.821	-
mean	0.298	0.294	0.327	0.357	0.254	0.258	0.296
1st Percentile	0.020	0.020	0.020	0.003	0.032	0.029	0.023
99th Percentile	3.183	3.335	3.929	4.487	2.100	2.650	3.089
\bar{N}^*	1.43×10^7	1.66×10^7	1.48×10^7	1.76×10^7	1.76×10^7	1.77×10^7	-

common observations, in time and space. Within this period OC-CCI global chl-*a* arithmetic average was $0.30 \pm 0.15 \text{ mg m}^{-3}$, the 1% percentile 0.023, and the 99% percentile 3.09 mg m^{-3} . Correlations between OC-CCI and precursor chl-*a* data sets were highly significant (probability value in significant test was < 0.01), strongly robust ($r > 0.95$), and, differences were relatively small ($\Delta_{u,RMS} < 0.15$, and, $|\delta| < 0.05$) (Table 2).

OC-CCI was more similar to single mission products, notably SeaWiFS, than the multi-mission merged data sets (Figure 2). Taylor diagram (Figure 2(a)), which illustrates a linear assessment of similarity between OC-CCI and precursors, suggests an obvious higher similarity of the OC-CCI with the SeaWiFS. But comparisons of OC-CCI with MERIS and MEaSUREs yielded an analogous result. The GC-GSM showed to be the least similar record with the OC-CCI. The non-linear-based MID (Figure 2(b)), however, agrees with the Taylor diagram, on that SeaWiFS is the most similar record to OC-CCI. However, this analysis places both GSM products, the GC-GSM and the MEaSUREs, as the most dissimilar records to the OC-CCI product. Nevertheless, generally, OC-CCI presented a positive bias in relation to all precursors except the GC-AVW, and a bigger unbiased difference, $\Delta_{u,RMS}$, when compared to both GSM products (Figure 2(c)).

SeaWiFS, which is the reference sensor for OC-CCI, exhibited the best global inter-comparison results, including the highest correlation ($r = 0.98$, when averaged through time), smallest difference ($\Delta_{u,RMS} = 0.097$), as well as the smallest bias ($\delta = -0.009$). Since SeaWiFS and OC-CCI use the same algorithm and wavelength bands to calculate chl-*a* concentrations, a high level of similarity between both data sets was expected. The small differences between the two products mainly arise from the different spatial resolution (see Section 3 for details on how the differences in resolution were handled), and from the fact that OC-CCI chl-*a* values are a merged product of values provided by SeaWiFS and two other missions (MERIS and MODIS).

The greatest differences were found between the OC-CCI and GSM chl-*a* values, that is, GC-GSM and MEaSUREs merged products. These two products had a smaller probability of containing the same information ($NI < 0.90$), a lower correlation ($r = 0.96$), and also the largest differences ($\Delta_{u,RMS} = 0.13$). Major differences between the OC-CCI and both GSM products are likely to be due to the use of a different algorithm (the GSM) to estimate chl-*a*. Nevertheless, the results from the two comparisons (i.e. the comparison between OC-CCI and both, GC-GSM and MEaSUREs products) differed from each other more than expected, given that both use the GSM algorithm and data source to

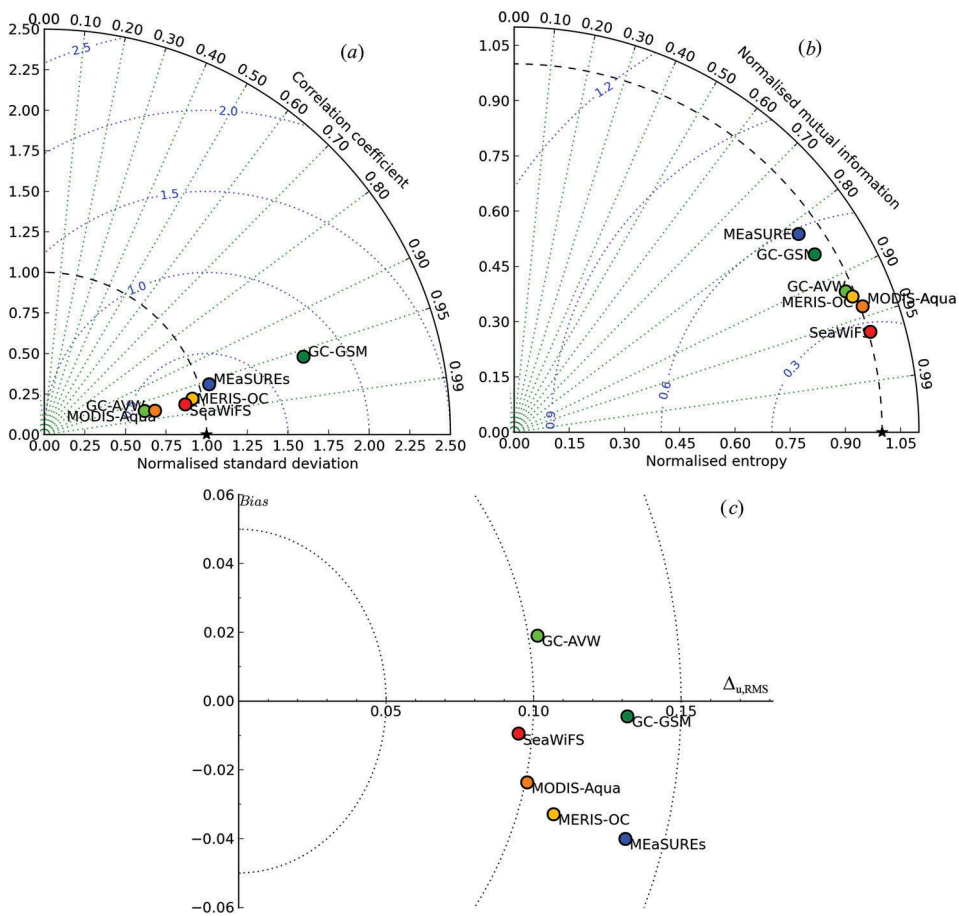


Figure 2. Taylor diagram (a), MID (b), and, target diagram (c) when comparing OC-CCI against precursor satellite-derived Chl data sets in a common period of observations (from January 2003 to December 2007). In Taylor and MI diagrams the star represents the perfect match with the OC-CCI record.

compute the chl-*a* values. For example, the value of δ (bias) was significantly different ($\delta_{GC-GSM} = -0.004$, $\delta_{MEaSUREs} = -0.04$). To understand this outcome it must be recalled that the two GSM products have considerable differences from each other (described in Section 2), such as the version of the original data, the atmospheric correction model, and spatial resolution. Further, the relationships between OC-CCI and MEaSUREs proved to be more constant throughout the common period between both data sets (September 1997 to July 2012) than the relationship between OC-CCI and GC-GSM for the same period, as seen by the wider spread of the standard deviation ratio between OC-CCI and GC-GSM for different months (Figure 3).

When comparing OC-CCI to the precursor data sets throughout 2003–2005, all metrics showed strong bi-annual and annual fluctuations, but the timing of the higher and lower peaks for each statistic varies with the metric, and data set compared against the OC-CCI product (Figure 4). Nevertheless, Figure 4 illustrates that GSM products stand out as the less similar products to OC-CCI, when assessing robustness (*r*), unbiased

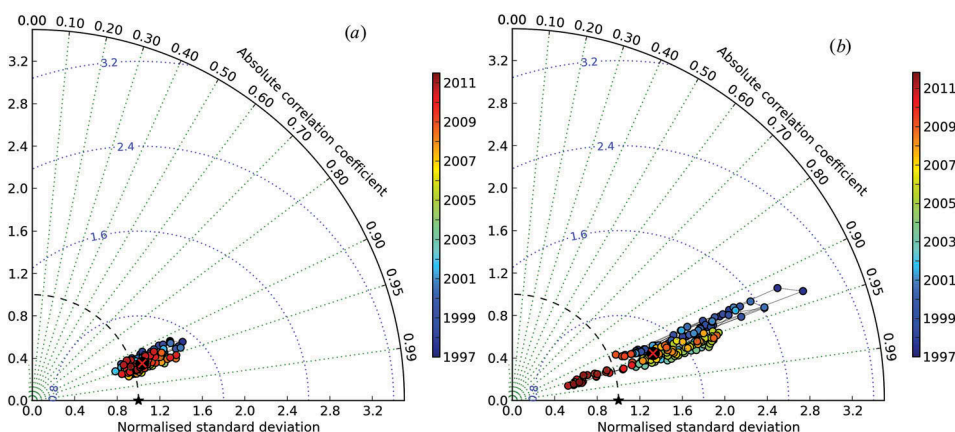


Figure 3. Taylor diagram when comparing OC-CCI with MEaSUREs (a), and when comparing with GC-GSM (b) throughout the common period each of the data sets (Table 1). The star represents the perfect match, as each data set is normalized with OC-CCI data.

difference ($\Delta_{u,RMS}$), and non-linear probability (NI). On the other hand, GC products presented a more positive δ (bias), and higher mean values (ϕ) than other compared records (Figure 4(a,e)). Further, merged multi-mission data sets showed a higher $\Delta_{u,RMS}$ annually during summer, while single mission data sets showed a strong semi-annual cycle of unbiased differences (Figure 4(c)).

The trends of all metrics between 2003 and 2007 (a common period to all data sets) indicate that the tendency of the relationship between OC-CCI and each precursor record considered is stable non-monotonic. The 5-year trends from the time-series of each statistics (i.e. ϕ , r , $\Delta_{u,RMS}$, δ , and NI) after removing the seasonal cycle were negligible (Table 3) and non-significant (probability value was bigger than 0.999). This was accompanied by a negligible trend of N , the matched number of observations between OC-CCI product and each precursor ($N_{trend} < 0.001\%$). Further, standard deviation of all statistics throughout the 5-year period did not suggest any significant variability of the parameters computed, indicating that similarity between the compared records remained relatively stable throughout the 5 years (Table 4).

4.2. Long-term analysis of the OC-CCI

As described in Section 3.2, temporal variability of $\Delta_{u,RMS}$ (when comparing OC-CCI against other data sets) is an indicator of the OC-CCI long-term consistency. All comparisons between OC-CCI and other data sets, including Pathfinder SST, showed that $\Delta_{u,RMS}$ varied strongly with the seasonal cycle (Figure 5). Comparison between OC-CCI and Pathfinder, however, showed a relatively higher $\Delta_{u,RMS}$ mean throughout the period considered ($\Delta_{u,RMS} = 1.7$) in contrast to comparisons between the chl-*a* data sets where $\Delta_{u,RMS} \leq 0.15$, which simply illustrates the difference between comparing two chl-*a* records, and comparing chl-*a* to a SST record. Further, the standard deviation of $\Delta_{u,RMS}$ ($s\Delta_{u,RMS}$) was also higher between SST and chl-*a* from OC-CCI ($s\Delta_{u,RMS} = 0.033$) than when considering the chl-*a* from OC-CCI and any other chl-*a* data set ($s\Delta_{u,RMS} < 0.012$). However, when only considering

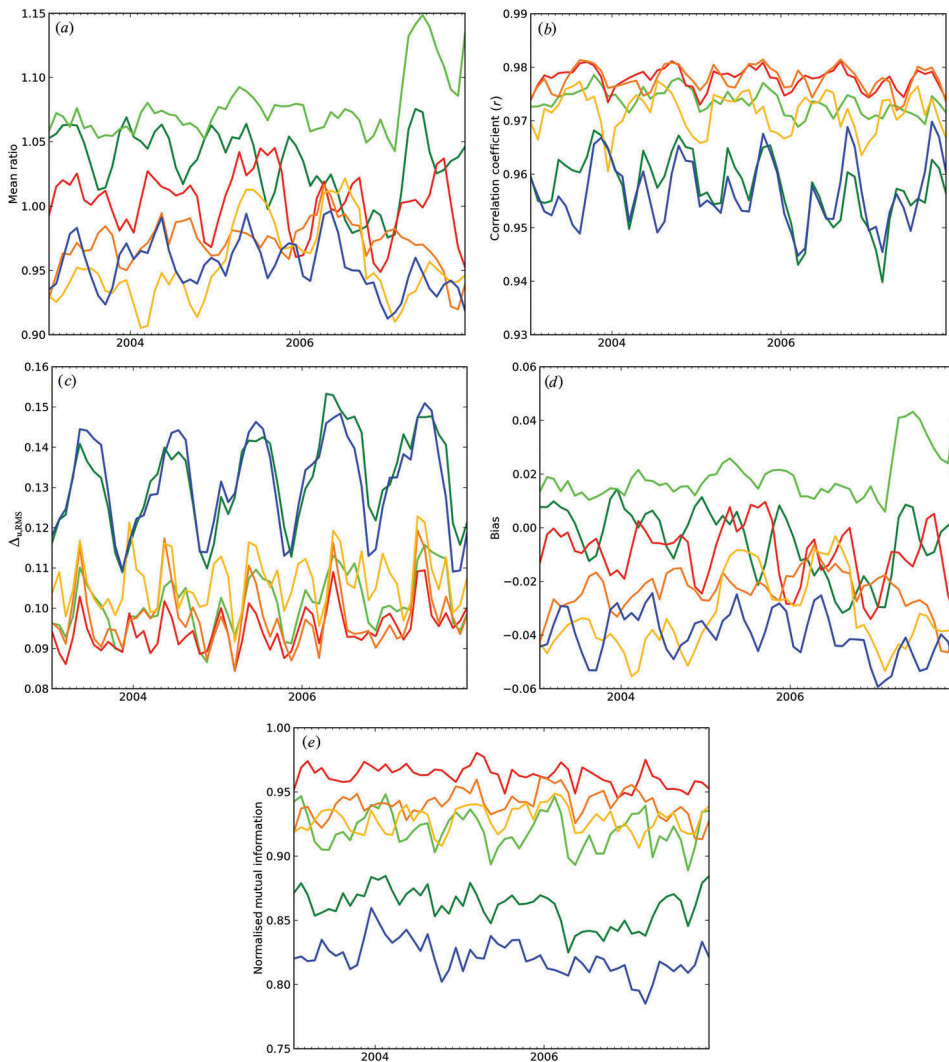


Figure 4. Time series of (a) ϕ (mean ratio), (b) r (correlation coefficient), (c) $\Delta_{u,RMS}$ (unbiased RMS difference), (d) δ (bias) and (e) NI (normalized mutual information) between January 2003 to December 2007, when comparing OC-CCI with: GC-GSM (green), GC-AVW (light green), SeaWiFS (red), MODIS-Aqua (orange), MERIS-OC (yellow), and MEaSUREs (blue).

other chl-*a* data sets, OC-CCI and SeaWiFS showed the most stable and consistent relationship with each other ($s\Delta_{u,RMS} = 0.005$, $s\Delta_{u,RMS} = 0.096$), whilst the GSM products showed less stable relationships ($\Delta_{u,RMS} > 0.14$, $s\Delta_{u,RMS} = 0.012$). Furthermore, during mid-2002 a big shift was observed in the $\Delta_{u,RMS}$ between SST and multi-mission chl-*a* products other than OC-CCI (Figure 5). This suggests that whatever changed the GC and MEaSUREs multi-mission products, might be absent from the OC-CCI data set since the SST record is independent from chl-*a* records. This big shift of $\Delta_{u,RMS}$, when comparing OC-CCI with other multi-mission data sets, is probably caused by the introduction of MERIS and MODIS-Aqua observations into the time series. The merging of several OC data sources started

Table 3. Trend after removing the seasonal cycle of mean ratio (ϕ), coefficient correlation (r), unbiased root mean square difference ($\Delta_{u,RMS}$), bias (δ), normalized mutual information (NI), and number of matched observations (N), when comparing OC-CCI with precursors during a common period for all data records (January 2003 to December 2007).

	SeaWiFS	MERIS	MODIS-Aqua	GC-AVW	GC-GSM	MEaSURES
ϕ	-2.48×10^{-4}	3.81×10^{-4}	4.12×10^{-5}	7.09×10^{-4}	-5.69×10^{-4}	-3.10×10^{-4}
r	-2.79×10^{-5}	-1.82×10^{-5}	-1.81×10^{-5}	7.44×10^{-5}	-1.80×10^{-4}	-4.28×10^{-5}
$\Delta_{u,RMS}$	-1.41×10^{-4}	1.68×10^{-4}	9.80×10^{-6}	2.35×10^{-4}	-3.24×10^{-4}	-1.79×10^{-4}
δ	1.28×10^{-4}	5.59×10^{-5}	4.27×10^{-5}	1.54×10^{-4}	2.73×10^{-4}	1.14×10^{-4}
NI	-1.70×10^{-4}	1.93×10^{-5}	3.15×10^{-5}	-1.34×10^{-4}	-3.20×10^{-4}	-3.94×10^{-4}
N	$-2.89 \times 10^{+3}$	$-1.73 \times 10^{+3}$	$-3.95 \times 10^{+3}$	-	-	-

All trends were found to be insignificant ($p > 99.9\%$).

Table 4. Standard deviation (SD) of mean ratio (ϕ), coefficient correlation (r), unbiased root mean square difference ($\Delta_{u,RMS}$), bias (δ), normalized mutual information (NI), and number of matched observations relative to the average (in percentage), when comparing OC-CCI with precursors during a common period for all data records, that is, from January 2003 to December 2007 (for all correlations $p < 0.01$).

SD	ϕ	r	δ	$\Delta_{u,RMS}$	NI	N (%)
SeaWiFS	2.40×10^{-2}	2.04×10^{-3}	1.08×10^{-2}	5.29×10^{-3}	7.94×10^{-3}	5.54
MERIS	3.07×10^{-2}	3.72×10^{-3}	1.37×10^{-2}	7.04×10^{-3}	1.00×10^{-2}	9.34
MODIS-Aqua	1.80×10^{-2}	2.33×10^{-3}	7.89×10^{-3}	7.55×10^{-3}	1.09×10^{-2}	7.45
GC-AVW	2.36×10^{-2}	2.21×10^{-3}	8.64×10^{-3}	6.97×10^{-3}	1.45×10^{-2}	6.44
GC-GSM	2.64×10^{-2}	6.12×10^{-3}	1.23×10^{-2}	1.16×10^{-2}	1.40×10^{-2}	6.51
MEaSURES	1.99×10^{-2}	6.09×10^{-3}	8.75×10^{-3}	1.19×10^{-2}	1.33×10^{-2}	6.91

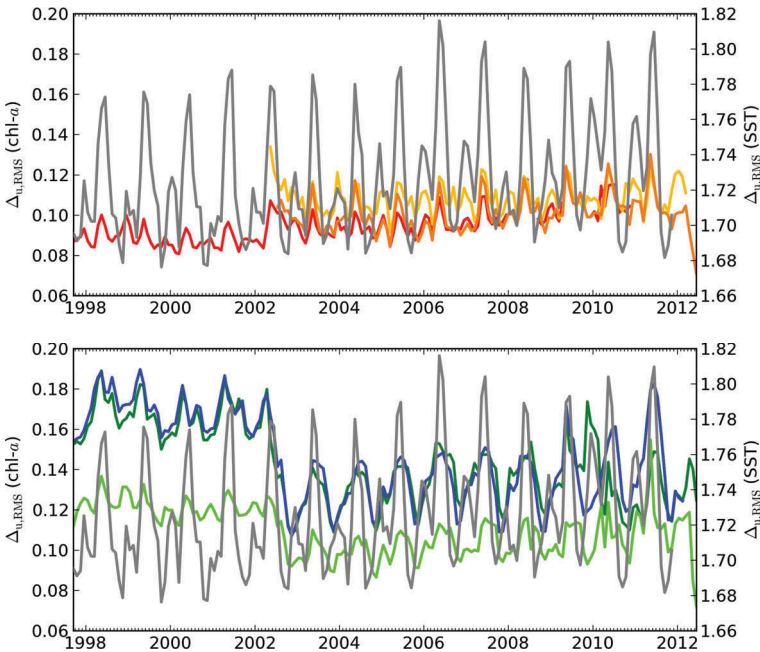


Figure 5. Time series of $\Delta_{u,RMS}$ between September 1997 to June 2012 when comparing (a) OC-CCI with single mission records, that is, SeaWiFS (red), MODIS-Aqua (orange) and MERIS-OC (yellow), and, (bottom panel) OC-CCI with multi-mission records (b), that is, GC-AVW (light green), GC-GSM (green), and, MEaSURES (blue). In both panels the comparison between SST (a measure of the ocean state independent from ocean colour observations) and OC-CCI is represented in grey and expressed in the right y-axis.

from mid-2002, with the inclusion of MERIS and MODIS-Aqua observations. Before this all multi-mission products (OC-CCI, GC, and MEaSUREs) only used SeaWiFS observations. Generally the main effects of additional data are positive, such as the increase of horizontal and temporal coverage, or the increase in the number of observations for a specific bin (which statistically makes any data set more robust). However, the addition of new observations may bring artefacts to the merged data set due to sensor divergences, which can affect the chl-*a* final product. The number of data contributed by each mission varied in time over the period but in mid-2002 the number of observations (N) increased significantly from a global monthly average of 1.4×10^7 from September 1997 to March 2002, to 1.8×10^7 monthly observations from July 2002 onwards for OC-CCI. Hence, this transitional period is crucial when considering OC-CCI consistency, or the consistency of any merged mission data set. Our results (shown in Figure 5) indicate that (1) OC-CCI did not change significantly its resemblance to SeaWiFS or SST in mid-2002, even though there was a sudden input of additional 0.4×10^7 observations per month in the OC-CCI product from MODIS-Aqua and MERIS; and (2) OC-CCI changed significantly compared with other merged data sets (GC-GSM, GC-AVW, and MEaSUREs) at this time. As SeaWiFS and SST products are independent of the additional data that occurred in mid-2002, these results strongly suggest that OC-CCI offers a greater degree of consistency when merging data than other multi-mission products used here.

5. Discussion

The OC-CCI Version 1 data set (released in December 2013) offers 22.9 billion (10^9) chl-*a* observations (an average of 127 million daily observations per month) spread in a 4.6 km global spatial grid over almost 15 years. Here, we compared the OC-CCI observations averaged in monthly composites (N = about 16 million per month) in order to increase spatial coverage, hence, the N used for comparison against six other similar data sets. By comparison, the World Ocean Database (WOA 2010), an initiative that gathers all kinds of ocean *in situ* measurements, includes in its records only 735 chl-*a* observations per month for the same period covered by OC-CCI. However, this coverage is not unique to the OC-CCI record, but to most global chl-*a* records derived from ocean colour remote sensing. SeaWiFS, for example, provided 4.7 million global daily observations per month, and a similar number of observations were reported for MODIS-Aqua and MERIS (Maritorena et al. 2010). Further, Maritorena et al. (2010) reported that merged satellite-derived products (e.g. GC or MEaSUREs) increased from around 70% to about 230% (depending on which single sensor product is compared) of the number of observations relative to the single mission products. Merging satellite data derived from different sensors is not so obvious when dealing with monthly composites, which can improve the SeaWiFS record global coverage by 6% (Maritorena et al. 2010). Our results indicate that, OC-CCI improves SeaWiFS coverage by at least about 10% when working with monthly composites.

Nevertheless, when combining data from different sources to obtain a more robust product, the quality of the outcome product as a time series may be degraded. SeaWiFS, MODIS-Aqua, and MERIS single-sensor data sets are quite consistent with each other during 2003–2007, with an average $\Delta_{u,RMS} \leq 0.14$ (reported by Djavidnia, Mélin, and Hoepffner 2010). Here, results indicate that OC-CCI is even more similar to all of these

single mission products within the common spatio-temporal frame ($\Delta_{u,RMS} \leq 0.11$, Table 2). Further, OC-CCI product showed to be more similar to single mission products than any of the other multi-mission merged products ($\Delta_{u,RMS} \leq 0.13$).

The values of $\Delta_{u,RMS}$ can be placed in a broader context by comparing satellite-derived chl-*a* products with *in situ* observations. Gregg and Casey (2004) reported that the Δ_{RMS} for SeaWiFS compared with *in situ* measurements is 0.310 ($N = 1689$), whilst, according to the SeaWiFS Bio-optical Archive and Storage System (SeaBASS) website (<http://seabass.gsfc.nasa.gov>), MODIS-Aqua data yields 0.308 ($N = 653$), and MERIS 0.323 ($N = 644$), when comparing the satellite observations against the SeaBASS *in situ* records. Maritorena et al. (2010), reported that multi-mission GSM chl-*a* estimates, yielded $\Delta_{u,RMS} = 0.399$ ($N = 778$) when compared with *in situ* observations. Since OC-CCI uses the same method and algorithm as the SeaWiFS chl-*a* product, one can expect the same quality of measurements from both products when compared to *in situ* observations.

When using linear and non-linear metrics, OC-CCI was found to be more similar to single mission records, particularly to the SeaWiFS record, and less to merged GSM products. The high similarity between OC-CCI and SeaWiFS is not surprising, as it reflects the fact that the SeaWiFS product serves as a reference in the OC-CCI data processing (Storm et al. 2013). For example, the band shifting and bias-correction of the R_{rs} are done with respect to SeaWiFS measurements. The OC-CCI record showed to have a positive bias against all other records, except the GC-AVW, where the merging technique used is a simple weighted average of the chl-*a* values retrieved by SeaWiFS, MODIS-Aqua, and MERIS (GlobColour 2010).

With respect to the long-term analysis, our results indicate that the OC-CCI record was the most consistent record throughout the time, particularly when considering both periods, before and after 2002. MERIS and MODIS-Aqua start to provide data in mid-2002, hence this is the crucial period for all multi-mission merged products that strive to keep a consistent multi-annual record. Our results indicate that OC-CCI is most consistent throughout the covered period since (1) when compared with an independent record (Pathfinder) no significant changes were observed in the unbiased difference variability ($s\Delta_{u,RMS}$), and (2) when compared with a dependent single mission record (SeaWiFS), $s\Delta_{u,RMS}$ was kept to a minimum for its full length. The biggest difference between merged records is in fact the technique used to merge observations from the different sensors. However, despite the multi-mission merged records assessed here use several different techniques to merge observations of the different sources, our results do not allow us to recommend a technique for long-term consistency, but they do suggest that bias correction may be recommended if temporal consistency is desired. Further, although both GSM products are shown to be the least similar products to OC-CCI, the two comparisons yield different results, probably due to the differences of both processing chains, as discussed by Maritorena et al. (2010). The dissimilarity level between GSM products and the OC-CCI may be influenced by the use of a completely different algorithm to calculate chl-*a*. The OC-CCI uses the same algorithm used by SeaWiFS record (i.e. OC4v6), which is quite similar to the algorithms used by other single mission records (Table 1). However, if the use of different algorithms would imply a significant dissimilarity between products, this would be reflected in our results, mainly expressed in the metric *bias* (e.g. Figure 2).

In conclusion, this study addresses the inter-comparison of available global satellite-derived chl-*a* data sets, considered an essential climate variable (GCOS 2011). Climate

variability and change motivate the creation of a long-term record of global near-surface chlorophyll concentration by merging time-limited, single-sensor missions, while minimizing the bias relative to each other. Here, OC-CCI is relatively similar to precursor records, but it can be distinguished by providing a larger number of observations, and, a better performance in long-term consistency.

Acknowledgments

This study is a contribution to the Ocean-Colour component of the Climate Change Initiative of the European Space Agency. The authors thank the Ocean Biology Processing Group of NASA, OrbView, GlobColour from ESA and University of California in Santa Barbara for the distribution of the data.

Disclosure statement

No potential conflict of interest was reported by the authors.

Funding

This work was supported by the European Space Agency project Ocean Colour - Climate Change Initiative.

ORCID

André Belo Couto  <http://orcid.org/0000-0002-2066-2277>

References

- Behrenfeld, M. J., R. T. O'Malley, D. A. Siegel, C. R. McClain, J. L. Sarmiento, G. C. Feldman, A. J. Milligan, P. G. Falkowski, R. M. Letelier, and E. S. Boss. 2006. "Climate-Driven Trends in Contemporary Ocean Productivity." *Nature* 444: 752–755. doi:10.1038/nature05317.
- Brewin, R. J. W., T. Hirata, N. J. Hardman-Mountford, S. J. Lavender, S. Sathyendranath, and R. Barlow. 2012. "The Influence of the Indian Ocean Dipole on Interannual Variations in Phytoplankton Size Structure as Revealed by Earth Observation." *Deep Sea Research Part II: Topical Studies in Oceanography* 77–80: 117–127. doi:10.1016/j.dsr2.2012.04.009.
- Casey, K. S., T. B. Brandon, P. Cornillon, and R. Evans. 2010. "The Past, Present and Future of the AVHRR Pathfinder SST Program." In *Oceanography from Space: Revisited*, edited by V. Barale, J. F. R. Gower, and L. Alberotanza, 273–287. Netherlands: Springer.
- Correa, C. D., and P. Lindstrom. 2013. "The Mutual Information Diagram for Uncertainty Visualization." *International Journal for Uncertainty Quantification* 3 (3): 187–201. doi:10.1615/Int.J.UncertaintyQuantification.2012003959.
- Couto, A. B., N. J. Holbrook, and A. M. Maharaj. 2013. "Unravelling Eastern Pacific and Central Pacific ENSO Contributions in South Pacific Chlorophyll-a Variability through Remote Sensing." *Remote Sensing* 5: 4067–4087. doi:10.3390/rs5084067.
- Djavidnia, S., F. Mélin, and N. Hoepffner. 2010. "Comparison of Global Ocean Colour Data Records." *Ocean Science* 6: 61–76. doi:10.5194/os-6-61-2010.
- Franz, B., S. W. Bailey, P. J. Werdell, and C. R. McClain. 2007. "Sensor-Independent Approach to the Vicarious Calibration of Satellite Ocean Color Radiometry." *Applied Optics* 46 (22): 5068–5082.
- GCOS. 2011. "Systematic Observation Requirements for Satellite-Based Data Products for Climate Update: Supplemental Details to the Satellite-Based Component of the Implementation Plan for

- the Global Observing System for Climate in Support of the UNFCCC (2010 Update).” Tech. rep. 154, 128. Geneva, Switzerland: World Meteorological Organisation (WMO).
- GlobColour. 2010. *Globcolour: An EO Based Service Supporting Global Ocean Carbon Cycle Research Product User Guide*, 85. Sophia-Antipolis, France: ACRI-ST.
- Gregg, W. W., and N. W. Casey. 2004. “Global and Regional Evaluation of the Seawifs Chlorophyll Data Set.” *Remote Sensing of Environment* 93: 463–479. doi:10.1016/j.rse.2003.12.012.
- Henson, S. A., J. L. Sarmiento, J. P. Dunne, L. Bopp, I. Lima, S. C. Doney, J. John, and C. Beaulieu. 2010. “Detection of Anthropogenic Climate Change in Satellite Records of Ocean Chlorophyll and Productivity.” *Biogeosciences* 7: 621–640. doi:10.5194/bg-7-621-2010.
- IOCCG. 2006. “Remote Sensing of Inherent Optical Properties: Fundamentals, Tests of Algorithms, and Applications.” In *Reports of the International Ocean-Colour Coordinating Group 5*, edited by Z. P. Lee. Dartmouth, Canada: IOCCG.
- IPCC. 2013. *Climate Change 2013: The Physical Science Basis: Contribution of Working Group I to the Fifth Assessment Report of the Intergovernmental Panel on Climate Change*, 1535. Cambridge: Cambridge University Press.
- Jolliff, J. K., J. C. Kindle, I. Shulman, B. Penta, M. A. M. Friedrichs, R. Helber, and R. A. Arnone. 2009. “Summary Diagrams for Coupled Hydrodynamic-Ecosystem Model Skill Assessment.” *Journal of Marine Systems* 76: 64–82. doi:10.1016/j.jmarsys.2008.05.014.
- Maritorena, S., O. H. F. d’Andon, A. Mangin, and D. A. Siegel. 2010. “Merged Satellite Ocean Color Data Products Using a Bio-Optical Model: Characteristics, Benefits and Issues.” *Remote Sensing of Environment* 114: 1791–1804. doi:10.1016/j.rse.2010.04.002.
- Maritorena, S., and D. A. Siegel. 2005. “Consistent Merging of Satellite Ocean Color Data Sets Using a Bio-Optical Model.” *Remote Sensing of Environment* 94: 429–440. doi:10.1016/j.rse.2004.08.014.
- Maritorena, S., D. A. Siegel, and A. R. Peterson. 2002. “Optimization of a Semianalytical Ocean Color Model for Global-Scale Applications.” *Applied Optics* 41 (15): 2705–2714. doi:10.1364/AO.41.002705.
- Mélin, F. 2014. “Ocean Colour Data Bias Correction and Merging.” Algorithm Theoretical Basis Document, 25. Ocean Colour Climate Change Initiative. http://www.esa-oceancolour-cci.org/?q=webfm_send/389
- Mélin, F., and G. Sclep. 2015. “Band Shifting for Ocean Color Multi-Spectral Reflectance Data.” *Optics Express* 23: 2262–2279. doi:10.1364/OE.23.002262.
- MERIS. 2011. *MERIS 3rd Data Reprocessing - Software and ADF Updates*, 84. http://earth.eo.esa.int/pcs/envisat/meris/documentation/meris_3rd_reproc/A879-NT-017-ACR_v1.0.pdf.
- Morel, A., Y. Huot, B. Gentili, P. J. Werdell, S. B. Hooker, and B. A. Franz. 2007. “Examining the Consistency of Products Derived from Various Ocean Color Sensors in Open Ocean (Case 1) Waters in the Perspective of a Multi-Sensor Approach.” *Remote Sensing of Environment* 111: 69–88. doi:10.1016/j.rse.2007.03.012.
- NASA. 2010. “Ocean Color Chlorophyll (OC) V6.” Accessed 18 July 2016. http://oceancolor.gsfc.nasa.gov/cms/atbd/chlor_a
- O’Reilly, J. E., S. Maritorena, D. Siegel, M. C. O’Brien, D. Toole, B. G. Mitchell, M. Kahru, et al. 2000. “Ocean Color Chlorophyll a Algorithms for Seawifs, OC2, and OC4: Version 4.” In *Seawifs Postlaunch Calibration and Validation Analyses*, edited by S. B. Hooker and E. R. Firestone, Vol. 11, 9–23. Greenbelt, MD: Goddard Space Flight Center.
- Sá, C., D. D’Alimonte, A. C. Brito, T. Kajiyama, C. R. Mendes, J. Vitorino, P. B. Oliveira, J. C. B. Da Silva, and V. Brotas. 2015. “Validation of Standard and Alternative Satellite Ocean-Color Chlorophyll Products off Western Iberia.” *Remote Sensing of Environment* 168: 403–419. doi:10.1016/j.rse.2015.07.018.
- Steinmetz, F., P.-Y. Deschamps, and D. Ramon. 2011. “Atmospheric Correction in Presence of Sun Glint: Application to MERIS.” *Optics Express* 19 (10): 9783–9800. doi:10.1364/OE.19.009783.
- Storm, T., M. Boettcher, M. Grant, M. Zühlke, N. Fomferra, T. Jackson, and S. Sathyendranath. 2013. *Product User Guide, Ocean Colour Climate Change Initiative*, 51. www.esa-oceancolour-cci.org/?q=webfm_send/317
- Taylor, K. E. 2001. “Summarizing Multiple Aspects of Model Performance in a Single Diagram.” *Journal of Geophysical Research: Atmospheres* 106: 7183–7192. doi:10.1029/2000JD900719.

WOA. 2010. "World Ocean Atlas 2009." Accessed 28 February 2015. <http://www.nodc.noaa.gov/OC5/WOA09/>

Yoder, J. A., and M. A. Kennelly. 2003. "Seasonal and ENSO Variability in Global Ocean Phytoplankton Chlorophyll Derived from 4 Years of Seawifs Measurements." *Global Biogeochemical Cycles* 17 (4): 1112. doi:[10.1029/2002GB001942](https://doi.org/10.1029/2002GB001942).